Soil Dynamics and Earthquake Engineering 63 (2014) 92–97

Contents lists available at ScienceDirect

Soil Dynamics and Earthquake Engineering

journal homepage: www.elsevier.com/locate/soildyn

Seismic base-isolation mechanism in liquefied sand in terms of energy

Takaji Kokusho

Department of Civil & Environment Engineering, Chuo University, Japan

ARTICLE INFO

Article history:
Received 22 July 2013
Received in revised form
20 January 2014
Accepted 24 March 2014
Available online 16 April 2014

Keywords:
Liquefaction
Seismic wave energy
Base isolation
Impedance ratio
Wave attenuation

ABSTRACT

Seismic base isolation effect in a liquefied sand layer was investigated based on soil properties measured in a series of undrained cyclic triaxial tests. Transmission of seismic wave in a soil model consisting of a liquefied surface layer and an underlying nonliquefied layer was analyzed in terms of energy, considering liquefaction-induced changes in S-wave velocity and internal damping. It was found that, between two different base-isolation mechanisms, a drastic increase in wave attenuation in the liquefied layer due to shortening wave length gives a greater impact on the base isolation with increasing thickness of the liquefied layer than the change of seismic impedance between the liquefied and nonliquefied layer. Also indicated was that cyclic mobility behavior in dilative clean sand tends to decrease the seismic isolation effect to a certain extent.

1. Introduction

During past earthquakes triggering seismic liquefaction, a seismic base-isolation effect was sometimes observed on building structures resting on liquefied ground. One of the first cases was apartment buildings in Kawagishi-cho, Niigata city, during the 1964 Niigata earthquake. Four-story RC buildings resting on very loose liquefiable sand settled and tilted considerably because they were directly on shallow foundations. There were seismometers at the base and roof of one of the buildings recording the earthquake motions as shown in Fig. 1, which demonstrates very clear base-isolation in which only low-amplitude long-period motions sustained after some seconds of S-wave shaking [1].

The number of such seismic records reflecting the liquefaction-induced base-isolation has increased since then. Wildlife site records shown in Fig. 2 during the 1987 Imperial Valley in California, USA, consist of not only ground motions but also in situ excess pore-water pressure [2]. Horizontal acceleration time histories at the surface show a peculiar motion reflecting cyclic mobility of liquefying sand. Another cyclic-mobility type acceleration records were observed in a vertical array in Kushiro harbor, in Hokkaido, Japan during the 1993 Kushiro-Oki earthquake [3]. Kobe Port-Island records during the 1995 Kobe earthquake were down-hole array strong motions observed in a man-made island, where top reclaimed decomposed granite sand and gravel of about 16 m thick liquefied extensively. The records at 4 different levels in Fig.3 clearly demonstrate deamplification in horizontal acceleration in the liquefied layer [4]. The wave energy flow was calculated based on the down-hole records, indicating that considerable energy dissipation occurred in the liquefied layer [5]. The cyclic-mobility type acceleration motion was also recorded at Kashiwazaki city during the 2007 Niigataken Chuetsu-oki earthquake [6]. During the 2011 Tohoku earthquake in Japan, quite a few records were obtained in liquefied sites, where long-lasting low acceleration motions by the M9.0 far-field subduction earthquake triggered liquefaction and cyclic-mobility type acceleration response in young-aged man-made soils e.g. [7]. The degree of base isolation in the above mentioned seismic records seems to differ from site to site, among which one in Kawagishi-cho during the 1964 earthquake seems to exhibit the most conspicuous base-isolation. Thus the manifestation of base-isolation seems to reflect the intensity of liquefaction associated with soil conditions and ground motions.

The effect of base isolation was also demonstrated by clear reduction in seismic energy, influencing structural damage of buildings resting on liquefied ground. During the 1964 Niigata earthquake, the RC buildings in Kawagishi-cho, previously mentioned, stayed perfectly intact, suffering no structural damage such as wall cracks or window-glass breakage [8]. During the 1995 Kobe earthquake, a viaduct highway route running through coastal liquefied man-made land in Kobe experienced little damage in superstructures directly by shaking, while another similar highway structures passing through inland nonliquefied areas, only a few kilometer apart, suffered severe damage in concrete columns by strong shaking [9]. During the 1999 Kocaeli earthquake in Turkey, building damage in a heavily damaged city, Adapazari, could be classified into shaking damage and liquefaction damage and the areas of the two types of damage did not overlapped [10].

E-mail address: kokusho@civil.chuo-u.ac.jp

http://dx.doi.org/10.1016/j.soildyn.2014.03.015
0267-7261/

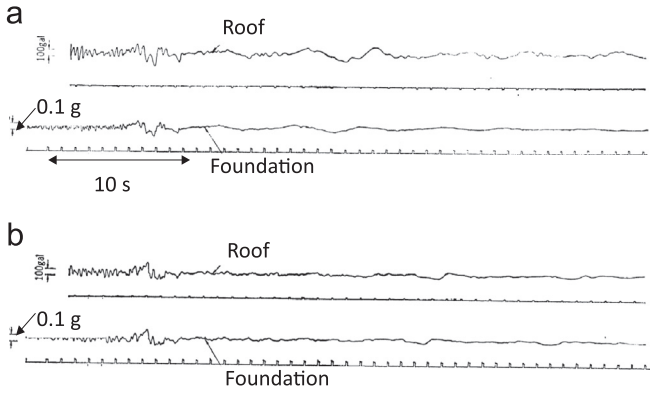

Fig. 1. Strong-motion records at Kawagishi-cho apartment building in Niigata city during 1964 Niigata earthquake [1].

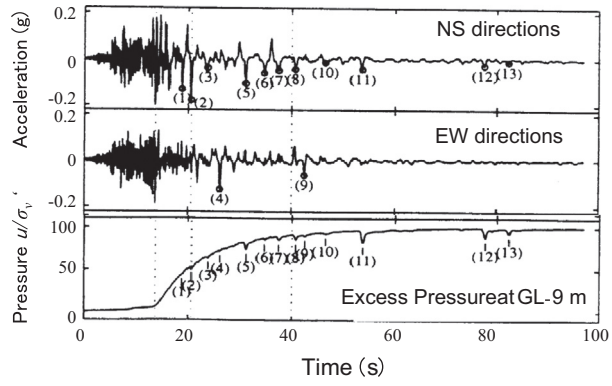

Fig. 2. Time histories of surface accelerations and subsurface excess pore pressure at Wildlife site during 1987 Imperial Valley earthquake [2].

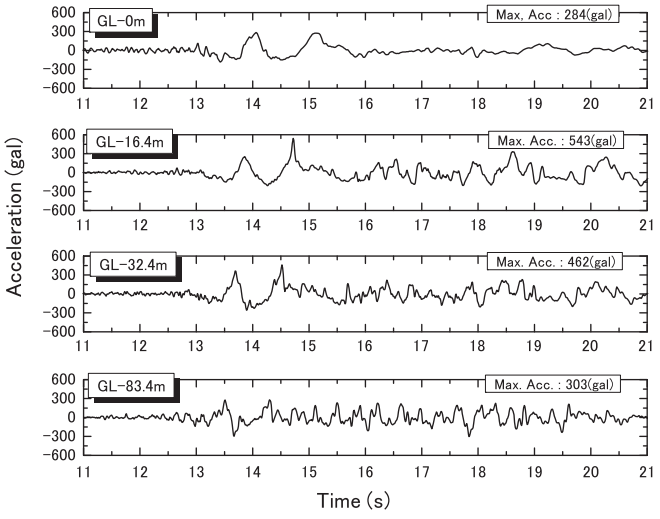

Fig. 3. Kobe Port Island down-hole array records: EW-direction [4].

It was pointed out during the 2004 Niigataken Chuetsu earthquake in Japan that roof tiles of Japanese wooden houses serve as an indicator if their foundation ground liquefied or not; no damage if liquefied [11]. More recently, almost no damage by seismic inertia force in superstructures has been seen during the 2011 Tohoku earthquake in liquefied areas in the Kanto plain in Japan.

Thus, the liquefaction-induced base-isolation is widely recognized not only in observed seismic records but also actual performance of structures. However, its basic mechanism has been discussed very scarcely, compared to liquefaction-induced geotechnical damage. In this paper, a uniform sand layer is considered as a simplified model to discuss the base-isolation mechanism under an idealized condition. In order to quantify liquefaction-induced variations of shear modulus and damping ratio, undrained cyclic triaxial test results are incorporated. Then, simple analyses based on a 1-dimesional wave propagation theory are conducted using the laboratory test results to evaluate the base-isolation effect in terms of energy in the liquefied layer.

2. Base-isolation mechanism

In order to evaluate liquefaction-induced base-isolation effect in a simple condition, let us consider a uniform fully-saturated sand layer shown in Fig. 4. It is assumed that, during an earthquake, liquefaction occurs in the upper portion with a thickness H but not in the lower part due to some reasons such as aging effect. Equivalent shear modulus and internal damping ratio corresponding to an induced strain amplitude before liquefaction are G_1 and D_1. Accordingly, S-wave velocity is $V_{s1}=\sqrt{G_1/\rho}$, using the soil density ρ. In the liquefied portion, G_1, D_1 and V_{s1} change to G, D and $V_s=\sqrt{G/\rho}$, whereas the properties in the nonliquefied part are assumed unchanged for simplicity, transforming the original uniform layer into a two-layer system of liquefied and nonliquefied layers as indicated in Fig. 4.

The wave equations in the two-layer system can be written as follows:

$$u_1 = A_1 e^{i(\omega t - k^* z)} + B_1 e^{i(\omega t + k^* z)} \tag{1}$$

$$u_2 = A_2 e^{i(\omega t - k_1^* z)} + B_2 e^{i(\omega t + k_1^* z)} \tag{2}$$

where u_1, u_2=horizontal displacements in the liquefied and nonliquefied layers, respectively, t=time, z=vertical coordinate upward starting from the layer boundary and $\omega=2\pi f$ is angular frequency. The complex wave numbers $k^*=\omega/V_s^*$ and $k_1^*=\omega/V_{s1}^*$ in the above equations are expressed by using the complex S-wave velocity, $V_s^*=(1+2iD)^{0.5}V_s$ and $V_{s1}^*=(1+2iD_1)^{0.5}V_{s1}$ in the liquefied and nonliquefied layers, respectively. Complex numbers A_1 and B_1 are amplitudes of upward and downward waves just above the boundary in the liquefied layer, respectively, and A_2 and B_2 are those just below the boundary in the nonliquefied layer. Using boundary conditions at the layer boundary ($z=0$) and at the ground surface ($z=H$), the amplitude ratio of A_1 to A_2 is expressed as

$$\frac{A_1}{A_2}=\frac{2}{(1+\alpha^*)+(1-\alpha^*)e^{-2ik^*H}} \tag{3}$$

where α^* is a complex impedance ratio defined by the equation

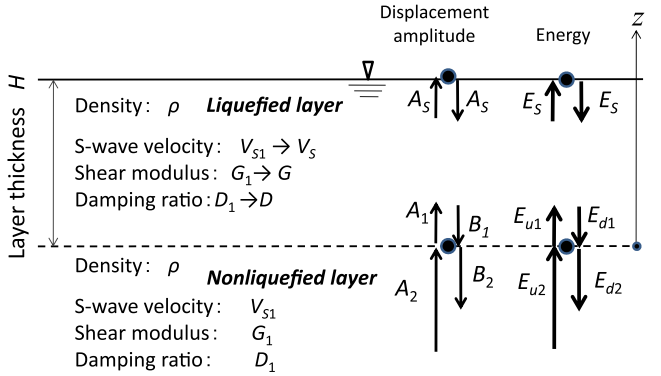

Fig. 4. 2-layer model of uniform sand transforming to upper liquefied and lower nonliquefied layers.